NASA TECHNICAL MEMORANDUM

NASA TM X-52959

NASA TM X-52959

COMPRESSIBLE FLOW ACROSS SHAFT FACE SEALS

by John Zuk, Lawrence P. Ludwig, and Robert L. Johnson
Lewis Research Center
Cleveland, Ohio

TECHNICAL PAPER proposed for presentation at Fifth International Conference on Fluid Sealing sponsored by The British Hydromechanics Research Association University of Warwick, Coventry, England, March 30-April 2, 1971

COMPRESSIBLE FLOW ACROSS SHAFT FACE SEALS

by John Zuk, Lawrence P. Ludwig,
and Robert L. Johnson

National Aeronautics and Space Administration
Lewis Research Center
Cleveland, Ohio
U.S.A.

E-6145

ABSTRACT

An analysis is presented for compressible fluid flow across shaft face seals and narrow slots. The analysis includes fluid inertia, viscous friction and entrance losses. Subsonic and choked flow conditions can be predicted and analyzed. The model is valid for both laminar and turbulent flows. Results agree with experiment and with solutions which are more limited in applicability. Results show that a parallel film can have a positive film stiffness under choked flow conditions.

INTRODUCTION

Shaft seal systems in advanced aircraft turbine engines will be operated at speeds, temperatures, and pressures higher than shaft seals currently used. Conventional face seals presently used in gas turbine engines are limited to sliding velocities of about 350 feet per second (110 m/sec), pressures of about 125 pounds per square inch (86 N/cm^2), and gas temperatures of 800° F (700 K)(ref. 1). Advanced engines, however, will require seals to operate to speeds of 500 feet per second (150 m/sec) (ref. 2), pressures to 500 pounds per square inch (340 N/cm^2) and temperatures to 1300° F (980 K)(ref. 3). For face seals operating at these conditions, a positive face separation (no rubbing contact) will be required

in order to achieve long life and reliability. A promising approach is the use of gas film seals with self-acting lift pads (see fig. 1 and Seal Description and Models).

Since the seals must be pressure balanced, a proper balance of the opening and closing forces must be achieved with a leakage gap that has tolerable mass leakage. The gap must be small enough so that the leakage is minimal but it must be large enough so that power dissipation, due to shear in the film, and face deformation are tolerable. Thus the design of the sealing gap is vital to seal performance and pressure distribution in the gap and mass leakage through the gap must be analyzed.

In this paper only the sealing dam portion of the seal will be analyzed. The classical viscous, isothermal, subsonic, compressible flow analysis for this problem is well known (e.g., see Gross, ref. 6). The pressure distribution and mass leakage have been calculated for the parallel film hydrostatic case. Carothers (ref. 7) has conducted compressible flow experiments in thin films of air which are flowing radially between parallel plates. The pressure distribution was found for both subsonic and supersonic axial entrance flows. Carothers' geometry, however, was representative of externally pressurized gas bearings rather than seals. Grinell (ref. 8) has theoretically and experimentally investigated compressible flow in thin passages and has shown agreement between theory and experiment. Müeller (ref. 9) included compressibility for the case where there was a restricted by-pass orifice flow into the parallel gap, but his analysis did not consider conditions which would yield choked flow in the gap. The textbook on mechanical face seals by Mayer (ref. 10) virtually

excluded face seal operation under conditions where fluid compressibility is important.

The objective of the report is to present a mathematical analysis of compressible fluid flow across shaft face seals and narrow slots. The analysis includes fluid inertia, viscous friction and entrance losses and thus describes both subsonic and choked flow conditions. For specified pressure ratios, film thicknesses, and friction factor variations with Reynolds number, which are used as parametric input, the output variables include mass and volume leakage flow rates, force, center of pressure and distributions of pressure, density, velocity, temperature and Mach number.

Seal Description and Models

A conventional face seal which is pressure (force) balanced is shown in figure 1. In this seal, the pressure drop occurs across a narrowly spaced sealing dam, and the force due to this pressure drop is balanced by a hydrostatic closing force and spring force. This configuration, however, has an inherent problem. For parallel sealing dam surfaces, the force caused by the pressure drop across the sealing dam is independent of film thickness for low Mach numbers; hence, there is no way of maintaining preselected film thickness which will allow tolerable leakage and still have noncontact operation. Since the force is independent of film thickness, the design also lacks axial film stiffness for sufficient dynamic tracking of the stationary nosepiece with the rotating seal seat. In order to operate adequately, the seal nosepiece must follow the seal seat

surface under all conditions without surface contact or excessive increase in film thickness, which would yield high leakage. Some of these conditions are axial runout, misalignment, thermal distortion, coning, and dishing.

A promising method of maintaining a preselected film thickness and achieving axial film stiffness is to add a self-acting gas bearing, such as shrouded Rayleigh step lift pads to the conventional rubbing contact pressure-balanced face seal (see fig. 2 for a sketch and refs. 4 and 5 for details of this concept, design and test results). Both the sealing dam force due to the pressure drop across the sealing dam and the self-acting lift pad (gas bearing) force are balanced by the hydrostatic and spring closing forces. The gas bearing has a desirable characteristic whereby the force increases with decreasing film thickness. If the seal is perturbed in such a way as to decrease the gap, the additional force generated by the gas bearing will open the gap to the original equilibrium position. In a similar manner, if the gap becomes larger, the gas bearing force decreases, and the closing force will cause the seal gap to return to the equilibrium position.

Some Models and Their Limitations

For subsonic flow, variable cross-sectional area, and Mach number $<1/\sqrt{\gamma}$ (all symbols are defined in Appendix A), the analysis of reference 11 can be used. This differential analysis finds a solution for the case when the viscous friction is balanced by the pressure drop and the fluid momentum change is negligible. For this condition the entrance pressure drop is small, hence $P_0 = P_1$, and $P_2 = P_3$ (see fig. 3). The flow is

nearly isothermal for the film thickness range studied. Neglecting rotation and inertia, it can be shown theoretically that the isothermal and adiabatic flow solutions on the average are identical (see ref. 12). The analysis of reference 11 yields the classical cubic dependence of mass flow on film thickness. Also, this analysis enables small tilts of the sealing dam surfaces to be studied. These small tilts simulate seal face deformations which can occur due to thermal, centrifugal, etc., effects.

For flow approaching Mach 1, i.e., choked flow, the inertia force neglected in reference 11 becomes important. Also, the flow behaves more as an adiabatic flow than an isothermal flow. The equations (partial differential equations) are relatively complex because of the nonlinearity of the inertia terms; thus an approximate analytical model must be used. In the approximate model presented here, the flow is analyzed as a quasi-one-dimensional flow utilizing a control volume integral analysis.

Since in gas film face seal applications there is seal seat rotation relative to the seal nosepiece, a question arises as to the validity of neglecting the centripetal inertia force which would affect the radial flow. This question was examined in reference 13. It was found that the circumferential rotational flow can be uncoupled from the radial pressure flow when the ratio of rotational velocity to pressure flow velocity is less than $1/\sqrt{R_e(h/\Delta R)}$. Rotational effects are important for calculating the viscous shear and power dissipation.

It should be pointed out that the flow in a gas film face seal is qualitatively quite different from the flow in an externally pressurized thrust bearing. Both operate with very small film thicknesses, usually less than 1 mil. However, gas film face seals are characterized by a

small $(R_2-R_1)/R_1$ ratio. Also, the inner cavity is a large supply reservoir. Hence, in gas film seals the reservoir pressure does not vary with film thickness. On the other hand, externally pressurized gas thrust bearings are characterized by a large $(R_2-R_1)/R_1$ ratio. (The large surface area is necessary for high load capacity.) In order to maintain positive film stiffness, compensating inlet flow restrictors are used. Because of these restrictors, the inlet pressure to the bearing varies significantly with film thickness. As a result of these differences, the flow regimes for the two cases are quite different. See reference 12 for a further discussion of this point.

QUASI-ONE-DIMENSIONAL FLOW ANALYSIS

As stated in the previous section, when the radial flow is close to choked or is choked at the exit, the viscous flow analysis in reference 11 is no longer valid. Fluid inertia, neglected in that analysis, becomes important. The rigorous inclusion of inertial terms necessitates the solution of nonlinear partial differential equations and is therefore not practical for engineering calculations; hence an approximate analytical model will be formulated which will be especially useful for calculating flow conditions near and at choking.

The geometry is shown in figure 3. Two parallel, co-axial, circular rings are separated by a very narrow gap. Rotational effects on the radial flow are negligible for most applications (ref. 13). A pressure differential exists between the ring's inner and outer radii. The cavities on either side (i.d. and o.d.) of the sealing dam are assumed to be

constant pressure reservoirs. For subsonic flow, reservoir conditions and the exit ambient pressure are specified. For choked flow, reservoir conditions and an exit Mach number of one are specified.

The analysis can be separated into two parts, which can then be considered separately. One part is an analysis of the seal passage itself, in which the flow is assumed to behave as a constant area, adiabatic flow with friction, while the other part is an analysis of the entrance flow. The analysis for these two regions will be described first followed by a discussion of the iterative procedure for the complete solution.

Constant Area Adiabatic Flow With Friction

It is assumed that the flow in the seal leakage flow region behaves as a constant area adiabatic flow with friction. A quasi-one-dimensional approximation is made wherein it is assumed that the flow properties can be described in terms of their cross-sectional averages.

The following assumptions have been made in the analysis:

1. The area expansion due to radius increase is neglected. (In most mainshaft face seals the i.d./o.d. is about 0.98)
2. The flow is adiabatic.
3. No shaft work is done on or by the system.
4. No potential energy is present such as elevation differences, etc.
5. The fluid behaves as a perfect gas.
6. The sealing surfaces are parallel.

With these assumptions, the flow is commonly known as Fanno line flow (ref. 15). This analysis is similar to that used by Grinnell (ref. 8)

for flow in thin passages. The governing equations when area changes are neglected are as follows:

1. Conservation of Mass

$$\dot{M} = \rho u A = \text{constant} \tag{1}$$

which reduces to:

$$\frac{d\rho}{\rho} + \frac{1}{2}\frac{du^2}{u^2} = 0 \tag{2}$$

2. Conservation of Energy

$$e + \frac{p}{\rho} + \frac{u^2}{2} = \text{constant}$$

or

$$h + \frac{u^2}{2} = \text{constant} \tag{3}$$

where h is the specific enthalpy. This can be written as

$$dh = C_p\, dT = -\frac{1}{2}\, du^2 \tag{4}$$

This equation can be reduced to

$$\frac{dT}{T} + \frac{(\gamma-1)}{2} M^2 \frac{du^2}{u^2} = 0 \tag{5}$$

where M is the Mach number, $u/\sqrt{\gamma RT}$

3. Equation of State

$$P = \rho RT \tag{6}$$

or

$$\frac{dP}{P} = \frac{d\rho}{\rho} + \frac{dT}{T} \tag{7}$$

4. Conservation of Momentum

$$-A\,dP - \tau_w\,dA_w = \dot{M}\,du \tag{8}$$

Now the following parameters will be introduced:

hydraulic diameter, D = $4A/\frac{dA_w}{dx}$

Darcy friction factor, f' = $\tau_w/\frac{\rho u^2}{2}$

It is assumed that the viscous effect can be represented by a mean friction factor. The mean friction factor depends on Reynolds number only and is a slowly varying function of Reynolds number for many flows, geometries, and conditions.

The set of equations (2, 5, 7, and 8) can be combined into a single equation in terms of the Mach number alone. Details of obtaining this equation can be found in Appendix B. The result is

$$\frac{4f'}{D}\,dX = \frac{(1-M^2)\,dM^2}{\gamma M^4\left(1+\frac{\gamma-1}{2}M^2\right)} \tag{9}$$

This equation can now be integrated from some location X_a, where the Mach number is M_a, to the location X_b, where the Mach number is M_b. By the use of partial fractions, the right-hand side of the above equation can be integrated to

$$\int_{M_a}^{M_b} \frac{(1-M^2)}{\gamma M^4\left(1+\frac{\gamma-1}{2}M^2\right)}\,dM^2 = B(M_a)-B(M_b) \tag{10}$$

where

$$B(M) = \frac{1}{\gamma}\,\frac{1-M^2}{M^2} + \frac{\gamma+1}{2\gamma}\ln\frac{\frac{\gamma+1}{2}M^2}{1+\frac{\gamma-1}{2}M^2} \tag{11}$$

Since the variation of f' with X is usually unknown, the integral of the left-hand side of equation (9) cannot be evaluated exactly. However, if f' is replaced by an appropriate mean value $\overline{f}'$, the integration may be performed.

$$\frac{4}{D}\int_{X_a}^{X_b} f'\,dX = \frac{4\bar{f}'}{D}(X_b - X_a) \tag{12}$$

The integration of equation (9) therefore yields

$$\frac{4\bar{f}'}{D}(X_b - X_a) = B(M_a) - B(M_b) \tag{13}$$

In the computer calculation, it is convenient to define a length

$$L_N = X_{MAX} - X_N \tag{14}$$

such that

$$\frac{4\bar{f}'}{D}(X_{MAX} - X_N) = \frac{4\bar{f}' L_N}{D} \tag{15}$$

$$\frac{4\bar{f}' L_N}{D} = B(M_N) \tag{16}$$

That is, L_N is the length of the seal (measured from X_N) for which the condition at the exit is sonic (choked). Note that $B(M = 1) \equiv 0$. It follows, if M_1 and M_2 are the Mach numbers at the inlet and exit of the seal, respectively, that

$$\Delta R = L_1 - L_2 \tag{17}$$

See figure 4.

The reservoir pressure and exit ambient static pressure are known. It is desirable to find the pressure at any point in the flow leakage passage as a function of Mach number. The flow is adiabatic. Thus the stagnation temperature is constant everywhere in the seal, i.e.,

$$T_{01} = T_{02} \tag{18}$$

or (ref. 15, p. 80)

$$T_1\left(1 + \frac{\gamma-1}{2} M_1^2\right) = T_2\left(1 + \frac{\gamma-1}{2} M_2^2\right) \tag{19}$$

From this relation, the continuity equation, the equation of state, and the definition of the Mach numbers, one obtains

$$\frac{P_1}{P_2} = \frac{M_2}{M_1}\sqrt{\frac{1 + \frac{\gamma-1}{2} M_2^2}{1 + \frac{\gamma-1}{2} M_1^2}} \tag{20}$$

Entrance Flow

If it is assumed that the flow in the entrance region is isentropic and adiabatic, the analysis is straightforward. The adiabatic energy equation is

$$h_o = h_1 + \frac{u_1^2}{2} \tag{21}$$

which can be written as

$$\frac{T_o}{T_1} = 1 + \frac{(\gamma-1) M_1^2}{2} \tag{22}$$

By use of the isentropic relation, P/ρ^γ = constant, and the equation of state, other inlet variables can be found knowing the sealed high pressure reservoir values, e.g.,

$$\frac{P_o}{P_1} = \left(\frac{T_o}{T_1}\right)^{\frac{\gamma}{\gamma-1}} = \left(1 + \frac{\gamma-1}{2} M_1^2\right)^{\frac{\gamma}{\gamma-1}} \tag{23}$$

$$\frac{\rho_o}{\rho_1} = \left(\frac{P_o}{P_1}\right)^{1/\gamma} = \left(1 + \frac{\gamma-1}{2} M_1^2\right)^{1/\gamma-1} \tag{24}$$

It is well known that entrance flows do not behave as isentropic flows but that an additional pressure drop is present due to viscous friction, turning losses, etc. A practical way of accounting for the entrance loss is to introduce an empirically determined velocity loss coefficient, C_L (see Appendix C). Hence equation (22) becomes

$$T_1 = \frac{T_o}{1 + \frac{(\gamma-1)M_1^2}{2C_L^2}} \tag{25}$$

while equation (23) becomes

$$P_1 = \frac{P_o}{\left(1 + \frac{(\gamma-1)M_1^2}{2C_L^2}\right)^{\frac{\gamma}{\gamma-1}}} \tag{26}$$

Under the entrance conditions discussed in Appendix C, the entrance velocity loss coefficient, C_L, is related to the head loss coefficient, k, commonly used in hydraulics by the following relation

$$k = \frac{1}{C_L^2} - 1 \tag{27}$$

Iteration Procedure

The procedure of solving the above equations is an iterative one. The solution is found using a computer program which appears in reference 12. In the iterative procedure, the first step is to solve for the minimum film thickness for which the flow is choked. If the actual film

thickness is less than this minimum value, the speed of the flow is less than sonic at the exit and the exit condition is $P_2 = P_3$. If the actual film thickness is greater than the minimum for choked flow, the exit flow is sonic and the exit condition is $M_2 = 1$, but the exit pressure is unknown. The details of the procedure are as follows:

Choked Film Thickness Evaluation

When the flow is just choked, it is known that $P_2 = P_3$ and $M_2 = 1$. By combining equation (26), the relation for P_0/P_1, with equation (20), the equation for $P_1/P_2 = (P_1/P_3)$ in the seal leakage passage, one obtains

$$\left(\frac{P_0}{P_1}\right)\left(\frac{P_1}{P_3}\right) = \frac{P_0}{P_3} = \frac{\left(1+\frac{\gamma-1}{2}\right)^{1/2}}{M_1} \frac{\left(1+\frac{\gamma-1}{2}\left(\frac{M_1}{C_L}\right)^2\right)^{\frac{\gamma}{\gamma-1}}}{\sqrt{1+\frac{1}{2}(\gamma-1)M_1^2}} \qquad (28)$$

Since P_0/P_3 is known, the Mach number M_1 can then be determined from this equation. Once the Mach number is known, all other flow quantities can be determined. The minimum choked film thickness is calculated as follows: (1) A film thickness h is assumed (chosen to be 1 mil in the computer program). (2) A Reynolds number is calculated from this film thickness. (3) This Reynolds number determines the flow regime, laminar or turbulent, and therefore the friction factor. ($\bar{f}' = \text{const.}/\text{Re}^n$, where the constant and exponent n are program inputs and depend on whether the flow is laminar or turbulent.) (4) A film thickness is then calculated by use of equation (16), i.e.,

$$B(M_1) = \frac{4\bar{f}'\Delta R}{D} = \frac{2\bar{f}'\Delta R}{h} \tag{29}$$

(For radial flow between co-axial parallel disks and parallel plates, the hydraulic diameter D = 2h.) If this h does not agree with the previous h, steps 2-4 are repeated until the h's agree. This defines the critical or minimum choked film thickness h*. It should be noted that equation (28) cannot be solved for all values of P_0/P_3, C_L and γ. Consequently, h* cannot be found. This condition arises for very low subsonic flows; hence the flow is assumed to be subsonic.

Subsonic Flow Case

For input film thickness less than the minimum choked film thickness, the flow is subsonic and the exit condition is $P_2 = P_3$. In this case it is convenient to use the length L_N defined by equation (14); that is, refer all quantities to a fictitious length of the seal for which the condition at the exit is sonic (choked). To start the iteration procedure, the entrance Mach number M_1 is assumed to be the same as for critical flow. All other quantities at the inlet are then calculated. The value of the friction parameter $B(M_1)$ is found from equation (11) and the choking length from equation (16), i.e., $L_1 = B(M_1)D/4\bar{f}'$. The length L_2 can be calculated from $L_2 = L_1 - \Delta R$ and then the friction parameter $B(M_2)$ from equation (11). Once $B(M_2)$ is known, the Mach number M_2 can be determined and, hence, the pressure P_2. This procedure is then repeated with a new Mach number M_1 until $P_2(M_1) = P_3$.

Choked Flow Case

For choked flow, the input film thickness is greater than the choking film thickness and the exit condition is $M_2 = 1$. As in the subsonic flow case, the iteration procedure begins with the entrance Mach number assumed to be the choking film thickness entrance Mach number. Again all entrance quantities are calculated. The friction factor $\bar{f}'$ is calculated from the Reynolds number and the friction parameter $B(M_1) = \frac{4\bar{f}'L}{D}$ is calculated from equation(11). The trial flow length, L, is calculated as

$$L = \frac{B(M_1)D}{4\bar{f}'} \tag{30}$$

If L is not equal to the true flow length, ΔR, the procedure is repeated with a new M_1 until L does agree with ΔR.

Calculation of Variables at Intermediate Points

Once the entrance conditions are known, the Mach number, temperature, velocity, and pressure are determined at each desired location, X_N, along the seal passage length in the following way:

1. L_N is found from equation (14).
2. $B(M_N)$ is calculated from equation (16).
3. M_N is found by an iterative solution of equation (11).
4. T_N is found from equation (19) where $T_2 = T^*$ and $M_2 = 1$, hence

$$T_N = \frac{\left(\frac{3+\gamma}{2}\right)T^*}{\left(1 + \frac{\gamma-1}{2}M_N^2\right)} \tag{31}$$

5. The velocity, U_N, is found from the Mach number definition.

6. The density is found from the mass conservation equation (1).

$$\rho_N = \rho_1 U_1 / U_N$$

7. The pressure is found from the perfect gas law, equation (6).

Computer Program

The computer program in reference 12 used to carry out this analysis is written in FORTRAN IV. The program is described in detail including all input and program variables and output options. Program listing and flow charts are presented and a sample problem with computer printout is given. The output can be either the U.S. Customary or International system of units.

RESULTS AND DISCUSSION

The computer program from reference 12 was used to carry out the quasi-one-dimensional flow analysis. By the use of this program, several problems have been solved. One such problem is a case used in the design study of reference 5. The sealed pressure and temperature were 65 psia (45 N/cm^2 abs) and 100° F (311 K), respectively. The exit ambient pressure was 15 psia (10.3 N/cm^{2}abs). The sealing dam radial width (seal leakage passage length) was 50 mils (0.127 cm). Figure 5 shows the calculated seal gas leakage as a function of film thickness, which ranges from 0.12 to 2 mils (0.0003 to 0.0051 cm).

The analysis agrees with the differential analysis of reference 11, which is the classical compressible viscous analysis, for subsonic viscous flow when the Mach number is less than $1/\sqrt{\gamma}$. As shown in figure 5, for film thicknesses less than 0.3 mil (8 m), the Mach number is less than

$1/\sqrt{\delta}$ = 0.845 and the leakage dependence on film thickness is the classical cubic dependence. The isothermal viscous flow model loses its validity when the Mach number exceeds $1/\sqrt{\delta}$. The present approximate model, however, is valid for both subsonic and choked flow. Figure 5 shows that for gaps larger than 0.3 mil (8μm) the leakage has a lesser than cubic dependence on film thickness. Note that choking occurs at a film thickness of 0.52 mils (13μm). The limiting case of orifice flow, in which the flow rate varies linearly with film thickness, would be achieved when the film thickness approaches the order of the sealing dam width of 50 mils (0.127 cm).

As indicated in figure 5, transition from laminar to turbulent flow occurs for a film thickness of approximately 1.3 mils (0.0033 cm). A Reynolds number, based on hydraulic diameter, equal to 2300 has been chosen to be the critical transition Reynolds number. This appears to be a universal critical transition Reynolds number for flows in ducts, pipes, and bearings. For laminar flow, a mean Fanning friction factor of $24/Re_{2h}$ was used. This friction factor is derived from the classical, viscous compressible flow solution in reference 12. For turbulent flow, the friction factor was chosen to be a constant equal to 0.0150, chosen from Egli's data (ref. 14) for annular flow. For the transition flow regime the exact nature of the flow, hence friction factor, is complex and not fully understood. The friction factor used for this flow regime is derived in reference 12 by assuming a smooth transition from the laminar friction factor to the turbulent friction factor. Reynolds numbers in the range from 2300 to 3000 are arbitrarily selected as the transition flow regime.

In order to check the validity of the model for choked flow and for a radial geometry representative of face seals, experiments were conducted at the Lewis Research Center.

Leakage flow was studied for two co-axial rings, 5.50 inches (14 cm) inner diameter, and 6.00 inches (15.2 cm) outer diameter, separated by a fixed parallel gap of 1.5 mils (0.0038 cm). The reservoir of 60.6 psia (41.8 N/cm^2 abs) pressure was held fixed and the exit pressure varied. Figure 6 shows a comparison of this analysis, the classical viscous subsonic flow differential analysis, and the radial flow experiment. Notice that the experiment shows that the flow does become choked. The maximum flow rate (choked) is 0.0176 lbm/sec (0.0080 kg/sec). The present analysis predicts a slightly higher mass flow but agreement is within 19 percent over most of the range. On the other hand, classical compressible viscous flow theory overestimates the flow rate considerably at all pressure ratios except very near one. The classical theory predicts no limiting mass flow. However, if the limit is chosen as the mass flow when the Mach number is unity, predicted flows are about 80 percent higher than observed experimentally for choked flow.

The analysis used a friction factor of $24/Re_{2h}$ over the laminar flow region. The good agreement in figure 6 indicates that it should be sufficient for engineering purposes to use this as a predictor. The important point is that it was derived analytically from classical compressible viscous flow theory. As is the case with duct flow, it appears to be nearly invariant with compressibility. Exact agreement could have been achieved if a different friction factor had been used. In this case almost exact agreement with the experimental curve would be achieved if $\bar{f}$ were

chosen to be $6/Re^{0.76}$; however, it may not be a reliable predictor for other experiments and applications.

There are many possible reasons for the disagreement between the analytical and experimental results. It is extremely difficult to maintain a uniform film thickness for the gap sizes of interest as small as 1.5 mils (0.0038 cm). Problems in clamping, machining tolerances, and distortions due to large pressure differentials result in experimental error. Another possible source of disagreement between theory and experiment could be due to area expansion, which the theory neglects. In the experiment, the inner diameter to outer diameter ratio is 0.92. Thus one could expect a lower flow rate than calculated. (Calculated mass flow is based on the arithmetic mean diameter.)

The theory also assumed isentropic entrance flow conditions. For large pressure differentials the entrance velocity is large enough to cause a substantial entrance pressure drop. The result of accounting for this entrance loss condition would also result in a decrease in mass flow. As illustrated in figure 6, an entrance velocity loss coefficient equal to 0.6 gave excellent agreement with experiment.

The radial flow experiment was repeated for two other reservoir pressures. The experimental results are shown in figure 7 and compared with the analysis. For a reservoir (sealed) pressure of 40 psia (27.6 N/cm^2 abs), the flow was laminar over the entire range studied. Agreement with the analysis assuming isentropic entrance conditions was within 18 percent. With an entrance loss coefficient of 0.6, agreement between analysis and experiment was within 5 percent.

For the 97.3 psia (67.1 N/cm^2 abs) reservoir pressure case, the transition Reynolds number of 2300 occurred for a pressure ratio of 0.87. The turbulent flow regime was set to begin at a Reynolds number of 3000 which occurred at a pressure ratio of 0.67. Using the mean friction factor of 0.015 from Egli's data yields excellent agreement with the analysis. However, for a 0.6 velocity entrance loss coefficient the flow was underestimated by 9 percent. Agreement in the laminar flow regime was excellent for the analysis with 0.6 entrance loss coefficient. The critical transition Reynolds number was calculated to occur at a pressure ratio of 0.8.

Figure 8 shows the 97.3 psia (67.1 N/cm^2 abs) reservoir pressure case experimental results compared with the analysis using a turbulent mean friction factor of $0.087/Re^{0.25}$. The inverse one fourth dependence on Reynolds number by the friction factor occurs for many fully developed turbulent flows. The analysis with isentropic entrance conditions overestimates the flow by 13 percent; however with an entrance loss coefficient of 0.6, the flow was underestimated by only 2.6 percent. In the laminar flow regime the curves are the same as in figure 7; agreement remains excellent.

Since shaft face seals are pressure balanced, it is necessary to know the sealing dam opening force which is found from

$$F = W \int_0^{R_2 - R_1} (P - P_{min.})\, dX \tag{32}$$

For classical viscous, compressible flow, the above equation is easily integrated in closed form and yields

$$F = \frac{2W(R_2-R_1)P_1\left[1-\left(\frac{P_2}{P_1}\right)^3\right]}{3\left[1-\left(\frac{P_2}{P_1}\right)^2\right]} - P_{min}(R_2-R_1) \quad (33)$$

Note that the opening force is independent of the fluid properties and film thickness. This gives the well known result that parallel surfaces yield no film stiffness. However, this is not the case when the classical compressible viscous flow theory is no longer valid. Figure 9 shows a plot of seal opening force versus film thickness obtained using the computer program in reference 12. Notice that for small film thickness (corresponding to M $1/\sqrt{\delta}$), the force is constant, as predicted by classical analysis. However as film thickness (and Mach number) increases, the force actually increases. This is a condition of negative film stiffness. It would be undesirable to operate in this region unless an auxiliary film stiffness generating device, such as self-acting lift pads, could make the overall seal stiffness positive. This negative stiffness may be one of the reasons why conventional gas film face seals "chatter" under certain high pressure conditions.

Also notice in figure 9 that the opening force attains a peak value, then sharply decreases with increasing film thickness. This sharp decrease indicates a high positive film stiffness which heretofore was not thought to be present for parallel surfaces.

The results using the analysis with an entrance loss coefficient of 0.6 are also shown in figure 9. The negative stiffness region has been

greatly reduced; however there is a larger region of positive film stiffness. A maximum film stiffness of about 57,800 lb_f/in. (102,000 N/cm) occurs at a film thickness of 0.6 mil (0.00152 cm). Notice that there is another possible negative stiffness region where the flow is in transition between laminar and turbulent flow. The uncertainty of the real flow behavior in this region may mean different behavior than that calculated. Positive film stiffness also occurs in the turbulent flow regime. Of course, in an actual seal design, the advantage gained by this added film stiffness must be weighed against the higher leakage flow resulting from choked flow operation.

Limitations of the Analysis

One of the limitations of this analysis is the neglect of the details of the flow in the entrance length. It is common in lubrication theory to neglect the entrance region entirely. This is correct for the slow viscous flows which characterize lubrication flows. However, when the flow becomes choked, the entrance velocities are high and it is possible that this neglect is improper.

The model developed herein may still be applied with good accuracy in cases where entrance effects are significant by using an entrance loss coefficient (see Eq. (25)-(27) and Appendix C). Fleming and Sparrow have shown in reference 16 the bulk of the entrance losses occur in a small region very close to the duct inlet. Laminar incompressible entrance loss coefficients have been calculated and measured for a variety of duct shapes (for example, refs. 16 and 17). Turbulent loss coefficients are not so

widely reported; however, they may be calculated for parallel plate channels from the information in reference 18. The values for k are generally less than 20 percent of those for laminar flow. Incompressible loss coefficients may be adequate for use with compressible flow (see Appendix C).

Also the use of the quasi-one-dimensional model can be justified by the good agreement with experiments and the short running time on the digital computer.

Seal Design Example

NASA has designed a seal with self-acting lift pads for potential use as a mainshaft seal in advanced gas turbine engines. This seal is described in references 4, 5, and 19. The sealing dam portion of this mainshaft face seal was designed and studied using the analysis.

Figure 10 shows the effect of sealing dam radial width on leakage flow film thicknesses from 0.1 mil (0.00025 cm) to 1 mil (0.0025 cm). The four radial dam widths used in the study were 5 mils (0.0127 cm), 20 mils (0.051 cm), 50 mils (0.127 cm), and 100 mils (0.254 cm). These plots illustrate that, from strictly a leakage point of view, the longest leakage path possible is most desirable. However,it is shown in reference 5 that the leakage path length must be compromised from a force balance point of view when surface deformations occur. Also shown in figure 10 is the leakage flow rate - film thickness relation for a 0.4 mil (0.001 cm) sealing dam radial width. Notice that at film thicknesses greater than 0.25 mils (0.000635 cm) the leakage coincides with the leakage values obtained for a knife edge using the theoretical orifice flow equation.

Also notice the linear variation of leakage flow with film thickness increase. For this narrow sealing dam width case when flow behaves as knife edge flow the velocity entrance loss coefficient is the same as the flow discharge coefficient used in orifice flow analysis.

Figure 11 shows mass leakage flow as a function of pressure ratio for a fixed gap of 0.4 mil (0.0001 cm) and varying sealing dam width. Notice the knife edge, as expected, has the largest leakage flow rate. These values have been calculated from the theoretical orifice flow equation. The computer program result for a sealing dam width of 0.4 mils (0.0001 cm) agreed with the theoretical orifice flow equation. As the sealing dam width increases, the critical pressure ratio for choking decreases as indicated by the sonic line in figure 11. Again the advantage of wider (longer) sealing dams is apparent.

Recent NASA sponsored tests (ref. 19) of a shaft face seal with self-acting lift augmentation have demonstrated the feasibility of operation at gas temperatures up to 1200° F (910 K), pressure differentials across the seal up to 250 psi (172 N/cm^2), and relative surface speeds up to 450 ft/sec (130 m/sec). These tests simulated the engine operating conditions such as takeoff, climb, cruise, and descent. The seal appears to be operating as predicted by the design analysis. Figure 12 shows the nosepiece seal assembly after the 120-hour endurance test. Figure 13 shows a closeup of the carbon nosepiece from the shaft face seal with self-acting lift pads after 320 hours of steady state endurance testing. The total time of testing on the carbon nosepiece was 338.5 hours. The pretesting lapping marks are still observable. A surface profile trace indicated that the average wear on the surface was less than 5 micro-

inches (0.13 μm). A few shallow scratches (50 to 100 microinches, 1 to 2 μm) were noticed. The test was concluded after 500 total hours of carbon nosepiece operation. The seal faces had encountered over 50 startups and shutdowns. The leakage rates varied from 11 to 32 SCFM (5.19×10^{-3} to 15.6×10^{-3} SCMS) with leakage generally averaging about 25 SCFM (1.18×10^{-3} SCMS). These leakage rates were close to those theoretically predicted.

SUMMARY OF RESULTS

An analysis has been presented for compressible fluid flow across shaft face seals. This quasi-one-dimensional integral analysis includes fluid inertia and entrance losses in addition to viscous friction which is accounted for by a mean friction factor. Subsonic and choked flow conditions can be predicted and analyzed. The model is valid for both laminar and turbulent flows. The following pertinent results were found:

1. Results agree with the classical subsonic compressible viscous flow theory for Mach numbers less than $1/\sqrt{\gamma}$. Excellent agreement with experiment is achieved if an entrance velocity loss coefficient of 0.6 is used in the laminar flow regime. A friction factor of 0.0150 in the analysis yielded good experimental agreement in the turbulent regime.

2. Near and at critical flow conditions (Mach number = 1), the analysis shows a negative film stiffness; whereas for choked flow the analysis predicts a high positive film stiffness. The analysis with an entrance loss coefficient of 0.6 yielded a maximum positive film stiffness of 57,800 lb_f/in. (102,000 N/cm) for a design problem studied. The choked flow results contrast to classical compressible viscous flow results which show no film stiffness for parallel surfaces.

APPENDIX A

SYMBOLS

A	area
B	friction parameter = $\frac{4\bar{f}'L}{D}$
C_L	velocity entrance loss coefficient
C_P	specific heat at constant pressure
D	hydraulic diameter = 2h
e	specific internal energy
F	sealing dam force
f'	Darcy friction factor
$\bar{f}'$	mean Darcy friction factor
$\bar{f}$	mean Fanning friction factor = $\bar{f}'/4$
h	film thickness (gap)
k	head loss coefficient
L	flow length
M	Mach number = $u/\sqrt{\gamma \mathbb{R} T}$
$\dot{M}$	mass flow
P	pressure
Q	volume leakage flow rate
r	radius
ΔR	sealing dam radial width (physical flow length), R_2-R_1
$\mathbb{R}$	gas constant = universal gas constant/molecular weight
Re	Reynolds number = $\rho u 2h/\mu$
T	temperature
u	velocity

W	flow width
X	radial coordinate direction
μ	absolute (dynamic) viscosity
γ	specific heat ratio, C_p/C_v
ρ	density
τ	shear stress

Subscripts

N	location along flow leakage length
0	sealed (reservoir) conditions
1	entrance conditions
2	exit conditions
3	ambient sump conditions

APPENDIX B

Friction Factor - Mach Number Relation

Equation (9) may be derived in the following way. From the equation of state (eq. (7)) and the energy equation, equation 5, one obtains

$$\frac{dP}{P} = \frac{d\rho}{\rho} + \frac{dT}{T} = \frac{d\rho}{\rho} - \left(\frac{\gamma-1}{2}\right) M^2 \frac{du^2}{u^2} \tag{B1}$$

Combining this with the mass conservation equation (eq. (2)) one obtains

$$\frac{dP}{P} = - \frac{1+(\gamma-1)M^2}{2} \frac{du^2}{u^2} \tag{B2}$$

Combining this with the momentum equation, equation 8, yields

$$\frac{2\gamma M^2 \overline{f'}}{D} dX - \left(\frac{1-M^2}{2}\right) \frac{du^2}{u^2} = 0 \tag{B3}$$

From the definition of the Mach number, $M^2 = u^2/\gamma R\, T$, and the energy equation, one obtains

$$\left(1 + \frac{\gamma-1}{2} M^2\right) \frac{du^2}{u^2} = \frac{dM^2}{M^2} \tag{B4}$$

Equations (B3) and (B4) then give

$$\frac{2\gamma M^2 \overline{f'}}{D} dX - \frac{(1-M^2)}{2\left(1+\frac{(\gamma-1)}{2} M^2\right)} \frac{dM^2}{M^2} = 0 \tag{B5}$$

from which equation (9) can be obtained, i.e.,

$$\frac{4\bar{f}'}{D}\,dx = \frac{(1-M^2)\,dM^2}{\gamma M^4\left(1+\frac{\gamma-1}{2}M^2\right)} \tag{B6}$$

APPENDIX C

Remark on Loss Coefficient

There are several effects which cause non-isentropic pressure drops in the face seal entrance region. Due to an abrupt geometric change at the seal passage entrance there is a non-uniform profile caused by flow turning, separated flow, and "vena contracta" effect which results in an entrance pressure drop. The pressure drop in the flow-development length is higher than that in the fully developed flow region because of two effects (ref. 16). The first effect is higher wall shear caused by higher transverse velocity gradients. The second effect is the momentum increase as the velocity distribution becomes less uniform.

The role of the entrance velocity loss coefficient may be better understood by considering the incompressible Bernoulli equation relating the stagnation reservoir pressure with the static and dynamic pressure at the seal entrance.

$$P_o = P_1 + \frac{1}{2}\rho_1 u_{1_{IDEAL}}^2 \tag{C1}$$

The actual velocity at the seal entrance is less than ideal; it can be expressed as

$$u_1 = C_L u_{1_{IDEAL}} \tag{C2}$$

Where C_L is the entrance velocity loss coefficient (see ref. 20).

Substitution of equation (C2) into (C1) and use of the Mach number definition yield

$$P_0 = P_1 + \frac{\gamma P_1 M_1^2}{2C_L^2} \tag{C3}$$

or

$$P_1 = \frac{P_0}{1 + \frac{\gamma M_1^2}{2C_L^2}} \tag{C4}$$

A binomial expansion of the denominator of the compressible entrance pressure equation (26) yields

$$\left[1 + \tfrac{1}{2}(\gamma-1)\frac{M^2}{C_L^2}\right]^{\frac{\gamma}{\gamma-1}} = 1 + \frac{1}{2}\frac{\gamma M^2}{C_L^2} + \frac{1}{8}\frac{\gamma M^4}{C_L^4} + \frac{\gamma(2-\gamma)}{48}\frac{M^6}{C_L^6} + \cdots \tag{C5}$$

The first two terms on the right-hand side strongly predominate for Mach numbers less than unity. For example, when $M/C_L = 1$ and $\gamma = 1.4$,

$$\left[1 + \tfrac{1}{2}(\gamma-1)\frac{M^2}{C_L^2}\right]^{\frac{\gamma}{\gamma-1}} = 1 + 0.70 + 0.18 + 0.02 + \cdots$$

The error is less than 11 percent if only the first two terms are used. The accuracy would be greater at lower Mach numbers. The first two terms of the expansion are the same as the denominator of the Bernoulli equation (C4) for a gas behaving as a quasi-incompressible fluid. Using this observation the relationship between the entrance velocity loss coefficient, C_L, and head loss coefficient, k, commonly used in hydraulics can be found. The incompressible Bernoulli equation with a head loss coefficient is

$$P_o - k\frac{\rho U_1^2}{2} = \frac{\rho_1 U_1^2}{2} + P_1 \tag{C6}$$

or

$$P_1 = P_o - (k+1)\frac{\rho U_1^2}{2}$$

$$= P_o - (k+1)\frac{\gamma P_1 M_1^2}{2} \tag{C7}$$

Comparing equation (C7) with equation (C3) yields

$$k = \frac{1}{C_L^2} - 1 \tag{C8}$$

This relation enables one to convert head loss coefficients reported in the literature to velocity loss coefficients C_L, which are more convenient to use in Mach number relations.

REFERENCES

1. Parks, A. J.; McKibbin, A. H.; Ng, C. C. W.; and Slayton, R. M.: Development of Mainshaft Seals for Advanced Air Breathing Propulsion Systems. Rep. PWA-3161, Pratt & Whitney Aircraft (NASA CR-72338), Aug. 14, 1967.

2. Shevchenko, Richard P.: Shaft, Bearing and Seal Systems for a Small Engine. Paper 670064, SAE, Jan. 1967.

3. McKibben, A. H.; and Parks, A. J.: Aircraft Gas Turbine Mainshaft Face Seals - Problems and Promises. Fourth International Conference on Fluid Sealing. Special Publication SP-2, ASLE, 1969, paper FICFS-28.

4. Johnson, R. L.; and Ludwig, L. P.: Shaft Face Seal With Self-Acting Lift Augmentation for Advanced Gas Turbine Engines. Fourth International Conference on Fluid Sealing. Special Publication SP-2, ASLE, 1969, paper FICFS-27.

5. Ludwig, L. P.; Zuk, J.; and Johnson, R. L.: Use of the Computer in Design of Gas Turbine Mainshaft Seals for Operation to 500 FT/SEC (122 M/SEC). Presented at 26th Annual Meeting of the National Conference on Fluid Power and the 10th Annual Meeting of the Fluid Power Society, Chicago, Ill., Oct. 13-15, 1970.

6. Gross, William A.: Gas Film Lubrication. John Wiley & Sons, Inc., 1962.

7. Carothers, P. R., Jr.: An Experimental Investigation of the Pressure Distribution of Air in Radial Flow in Thin Films Between Parallel Plates. MS Thesis, U.S. Naval Post Grad. School, Monterey, Calif., 1961.

8. Grinnell, S. K.: Flow of a Compressible Fluid in a Thin Passage. Trans. ASME, vol. 78, no. 4, May 1956, pp. 765-771.

9. Müller, Heinz K.: Self Aligning Radial Clearance Seals. Proceedings of the Third International Conference on Fluid Sealing, British Hydromechanics Research Assoc., Cambridge, England, Apr. 3-5, 1967, paper H6.

10. Mayer, E. (B.S. Nau, trans.): Mechanical Seals. American Elsevier, 1970.

11. Zuk, John; and Smith, Patricia J.: Computer Program for Viscous, Isothermal Compressible Flow Across a Sealing Dam with Small Tilt Angle. NASA TN D-5373, 1969.

12. Zuk, J.: Quasi-One-Dimensional Compressible Flow Across a Sealing Dam - Analysis and Computer Program. NASA Technical Note (in process).

13. Zuk, John; and Ludwig, Lawrence P.: Investigation of Isothermal, Compressible Flow Across a Rotating Sealing Dam. I - Analysis. NASA TN D-5344, 1969.

14. Egli, Adolf: The Leakage of Gases Through Narrow Channels. J. Appl. Mech., vol. 4, no. 2, June 1937, pp. A-63 - A-67.

15. Shapiro, Ascher H.: The Dynamics and Thermodynamics of Compressible Fluid Flow. Vol. I. The Ronald Press Co., 1953.

16. Fleming, David P.; and Sparrow, E. M.: Flow in the Hydrodynamic Entrance Region of Ducts of Arbitrary Cross Section. J. Heat Transfer, vol. 91, no. 3, Aug. 1969, pp. 345-354.

17. Lundgren, T. S.; Sparrow, E. M.; and Starr, J. B.: Pressure Drop Due to the Entrance Region in Ducts of Arbitrary Cross Section. J. Basic Eng., vol. 86, no. 3, Sept. 1964, pp. 620-626.

18. Deissler, Robert G.: Analysis of Turbulent Heat Transfer and Flow in the Entrance Regions of Smooth Passages. NACA TN 3016, 1953.

19. Povinelli, V. P.; and McKibbin, A. H.: Development of Mainshaft Seals for Advanced Air Breathing Propulsion Systems - Phase II. Rep. PWA-3933, Pratt & Whitney Aircraft (NASA CR-72737), June 23, 1970.

20. Sabersky, Rolf H.; and Acosta, A. J.: Fluid Flow. Macmillan Co. 1964.

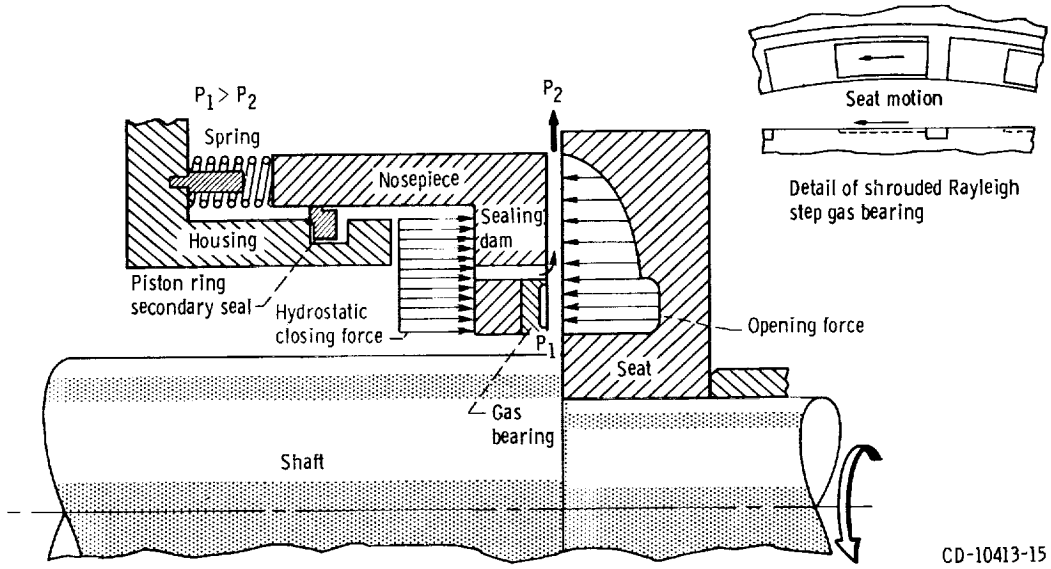

Figure 1. - Pressure-balanced face seal with a gas bearing added for axial film stiffness.

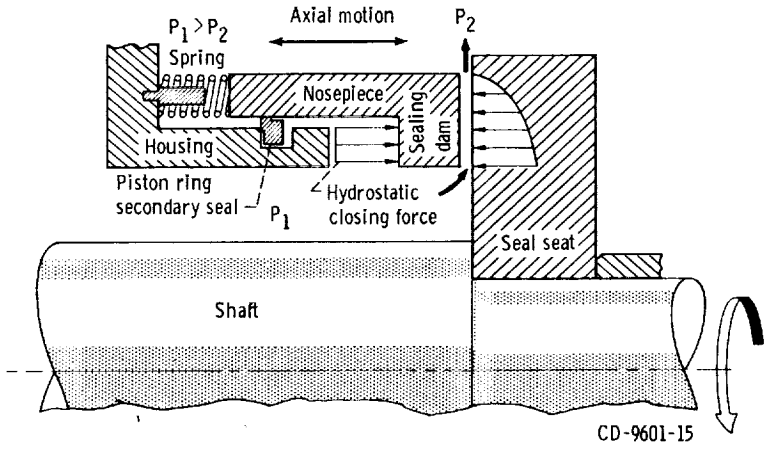

Figure 2. - Pessure-balanced face seal with no axial film stiffness.

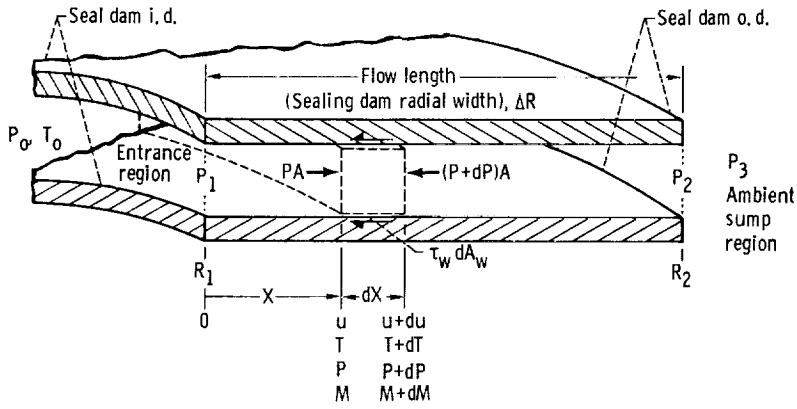

Figure 3. - Model and notation of sealing faces including control volume for quasi-one-dimensional flow.

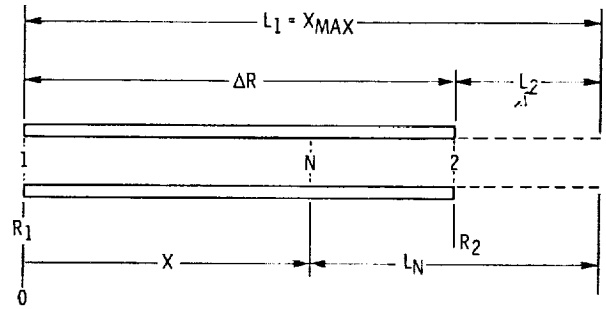

Figure 4. - Lengths and stations used in the analysis. (Subsonic case is shown.)

E-6145

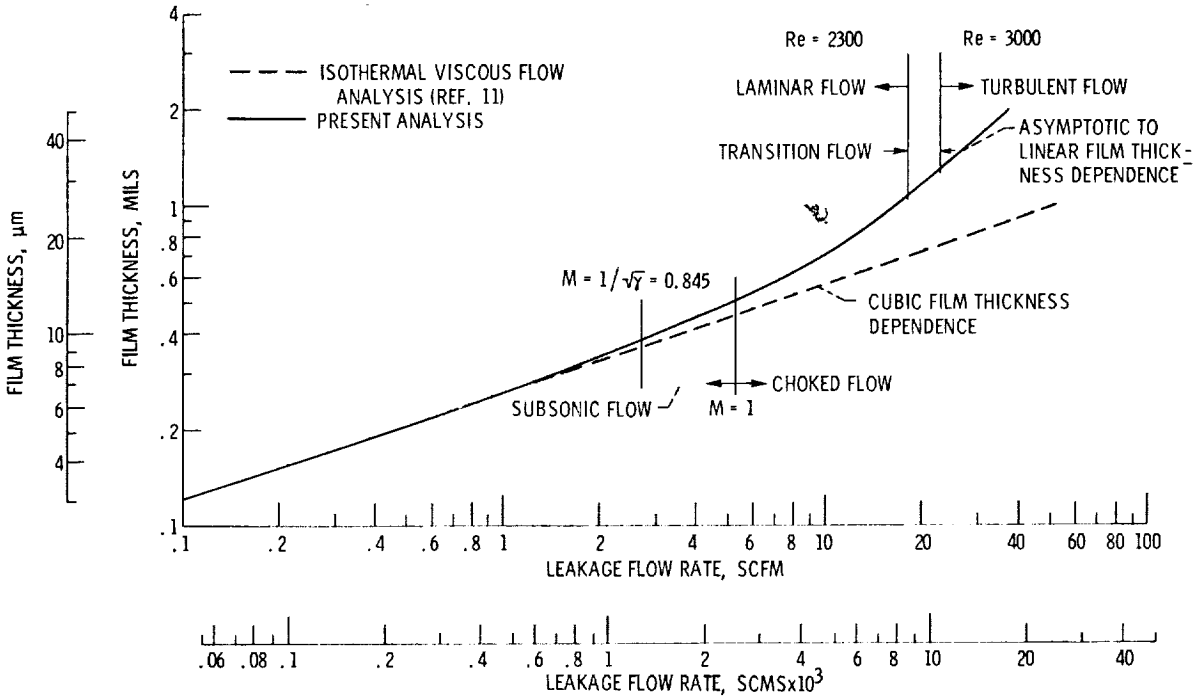

Figure 5. - Seal gas leakage versus film thickness for parallel sealing dam surfaces. Radial dam width, ΔR, 50 mils (0.130 cm); sealed air pressure, P_0, 65 psia (45 N/cm^2 abs); sealed air temperature, T_0, 100° F (310 K); sump pressure, P_3, 15 psia (10 N/cm^2 abs).

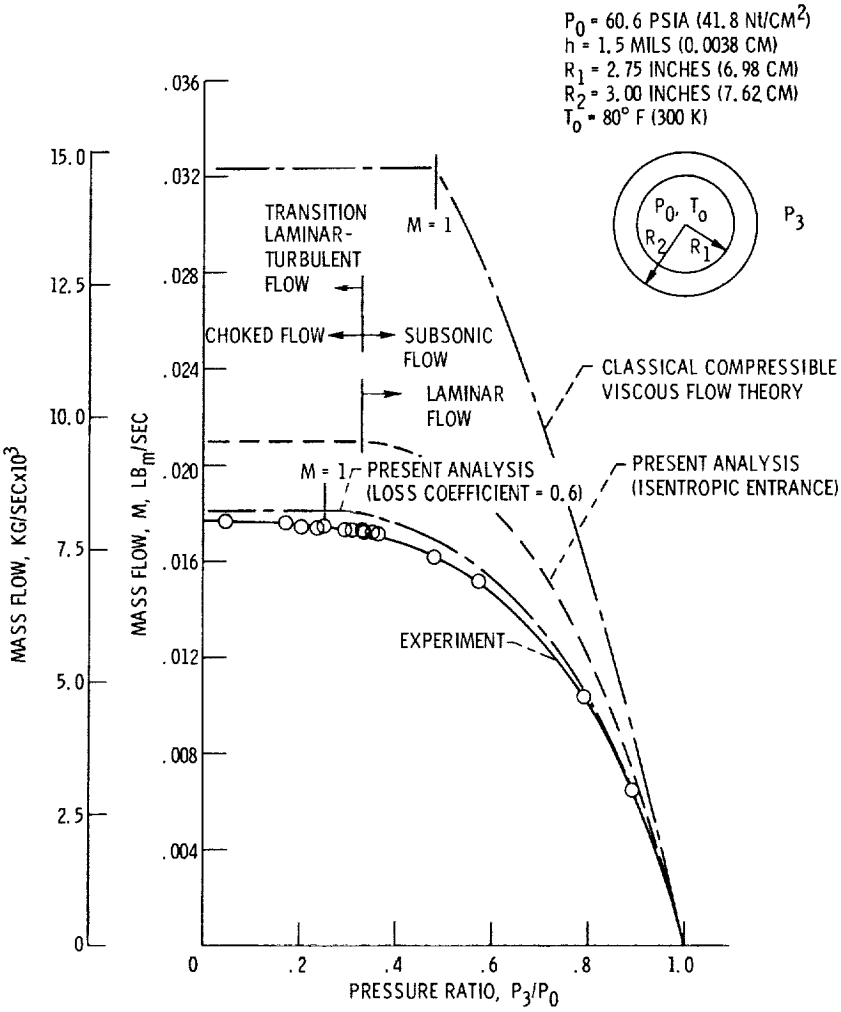

Figure 6. - Comparison of classical viscous flow theory and present analysis with radial flow experimental results.

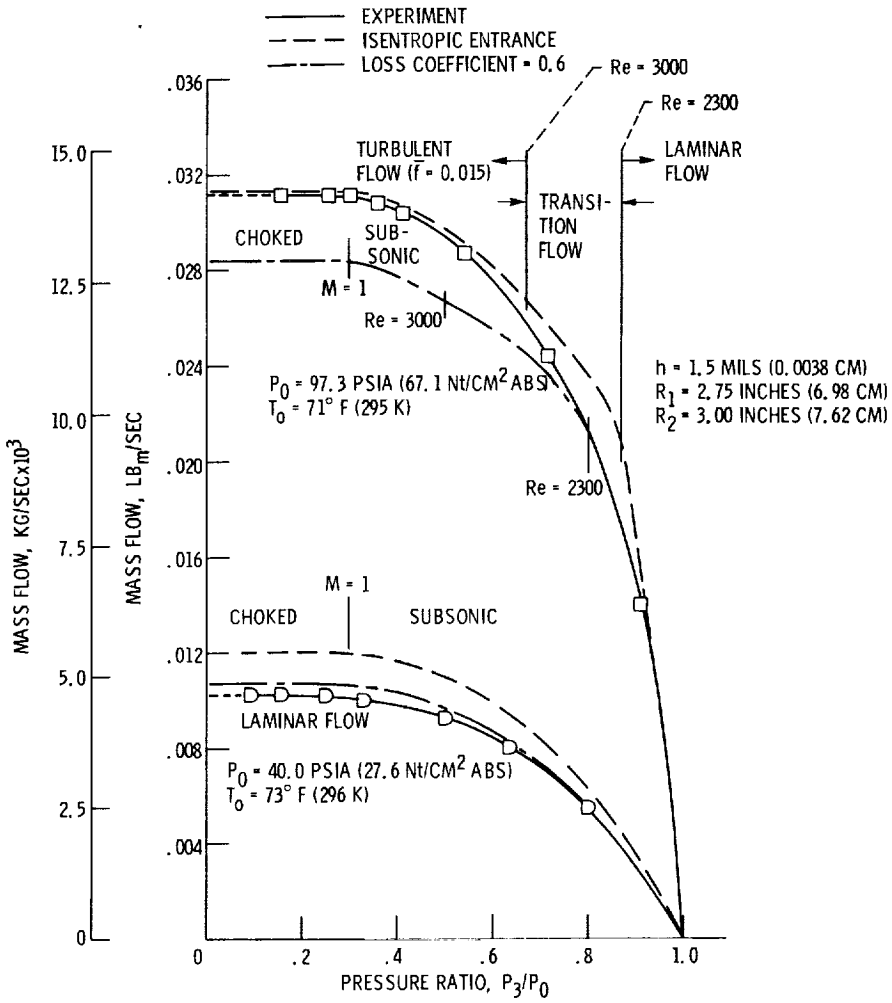

Figure 7. - Comparison of present analysis with radial flow experimental results.

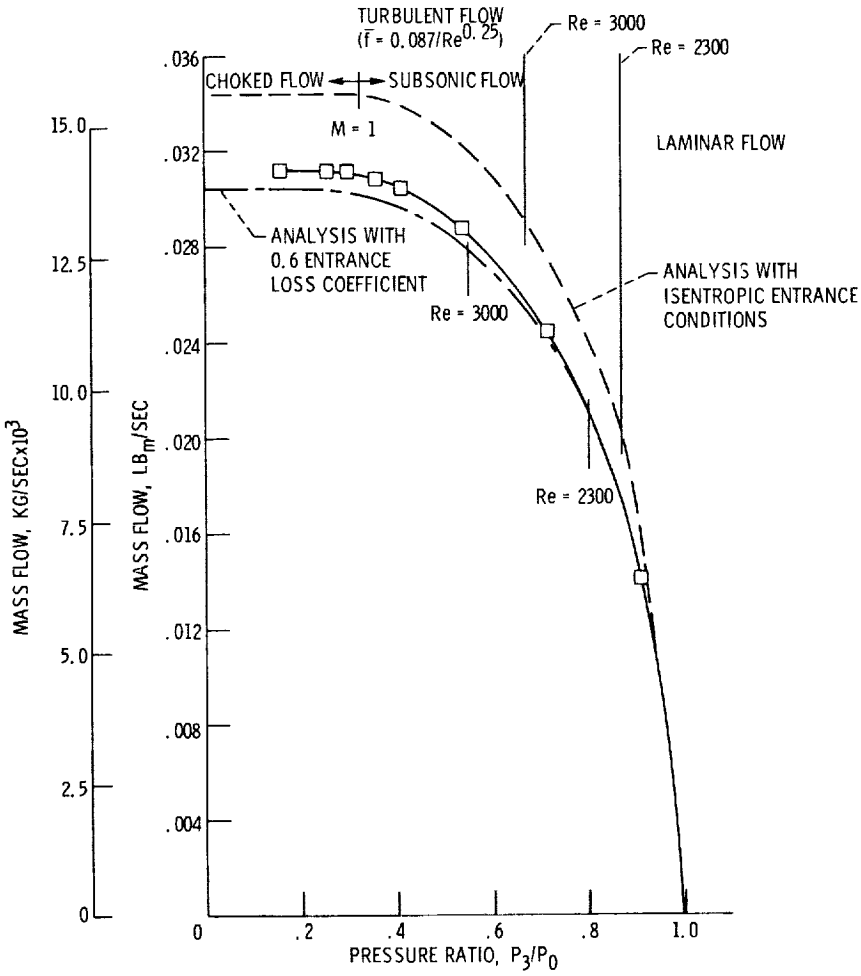

Figure 8. - Comparison of present analysis using 0.087/Re$^{0.25}$ turbulent friction factor with radial flow experimental results; P_0, 97.3 psia (67.1 N/cm^2 abs); T_0, 71° F (295 K); gap, 1.53° mils (0.0039 cm); R_1, 2.75 in. (6.98 cm); R_2, 3.00 in. (7.62 cm).

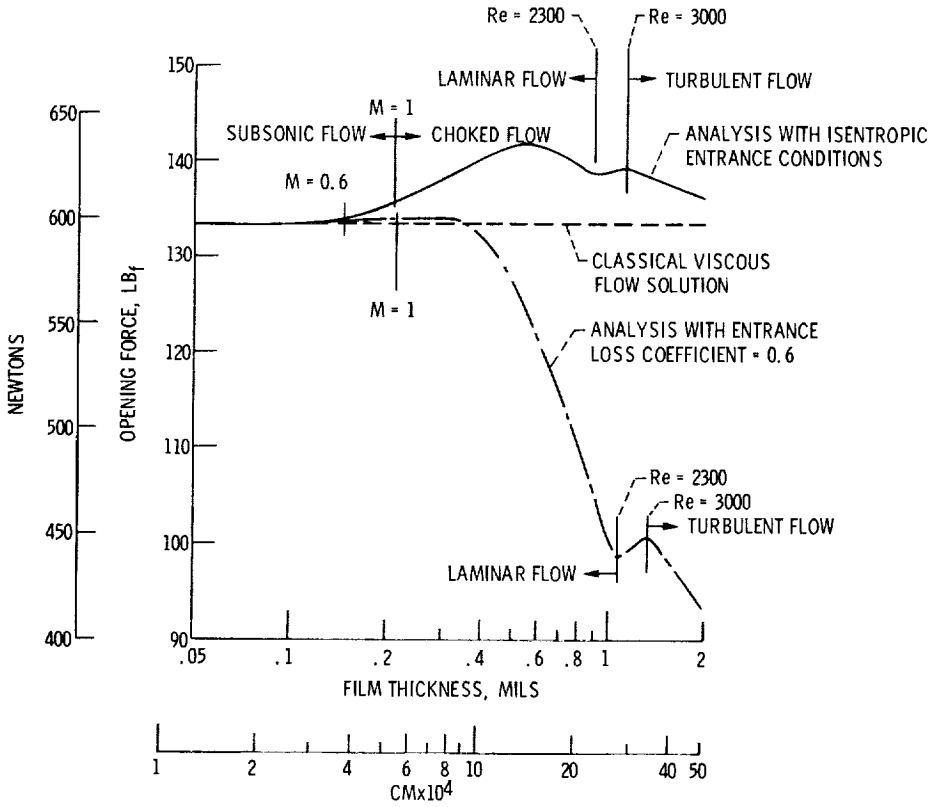

Figure 9. - Sealing dam opening force plotted as function of film thickness for parallel surfaces comparing classical theory with present analysis with both isentropic and 0.6 entrance loss coefficient; P_0, 215 psia (148 N/cm^2 abs); P_3, 15 psia (10.3 N/cm^2 abs); T_0, 800° F (700 K); ΔR, 50 mils (0.127 cm).

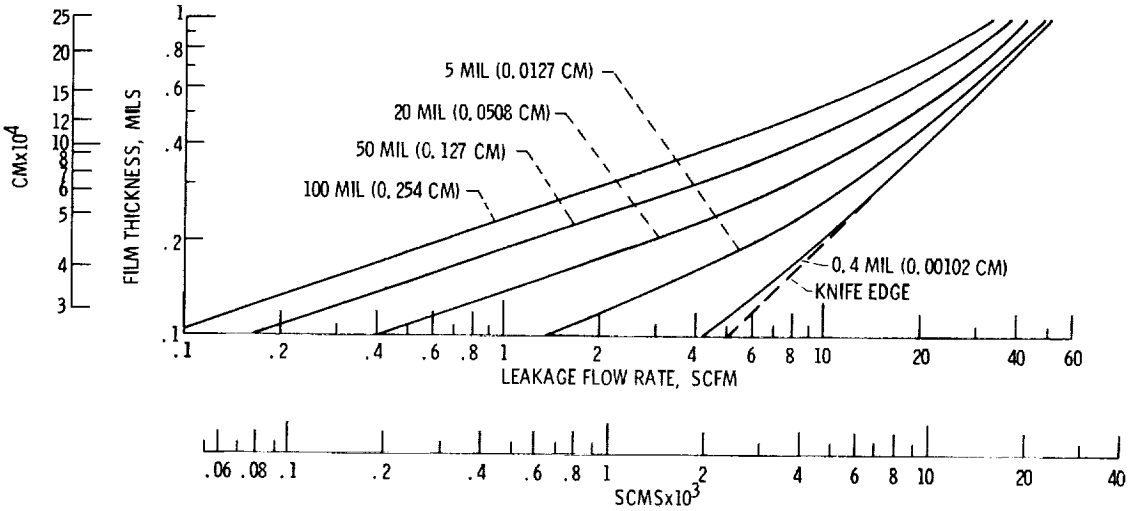

Figure 10. - Effect of seal face radial length on seal leakage; parallel sealing faces; sump pressure, P_3, 15 psia (10.3 N/cm^2 abs); sealed pressure, P_0, 215 psia (148 N/cm^2 abs); sealed gas temperature, 800° F (700 K).

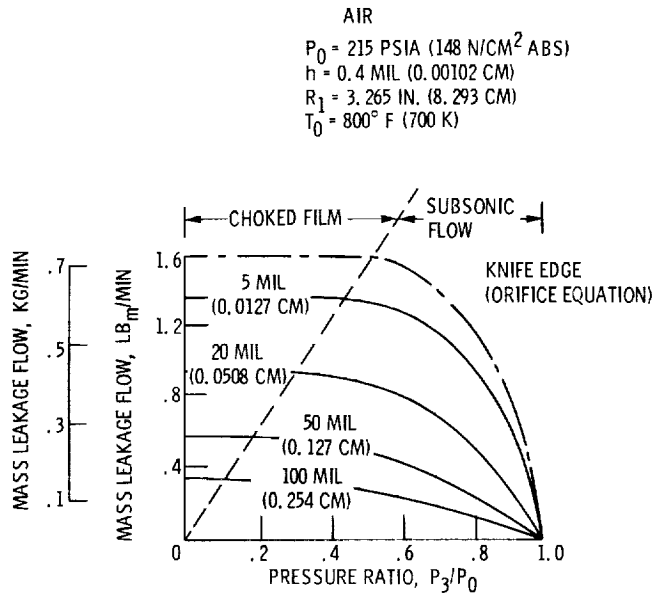

Figure 11. - Mass leakage as a function of pressure ratio for various sealing dam radial lengths.

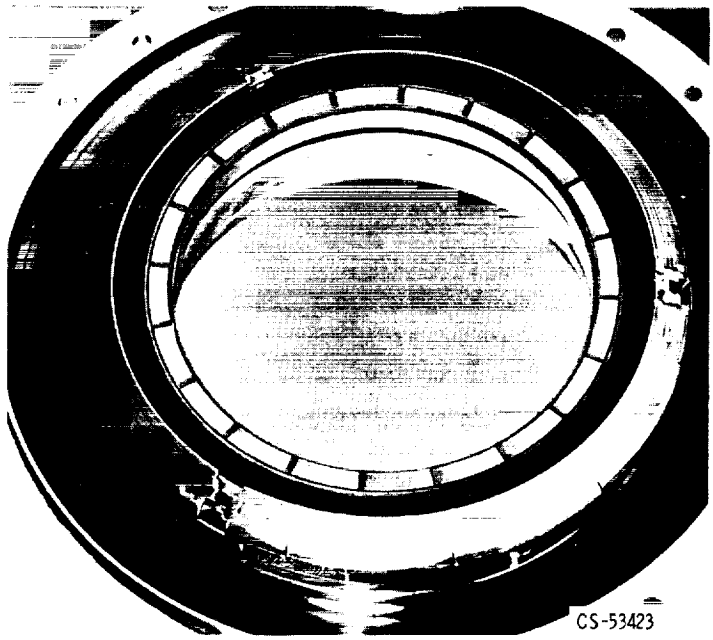

Figure 12. - Gas-film seal assembly nosepiece after 120-hour endurance test.

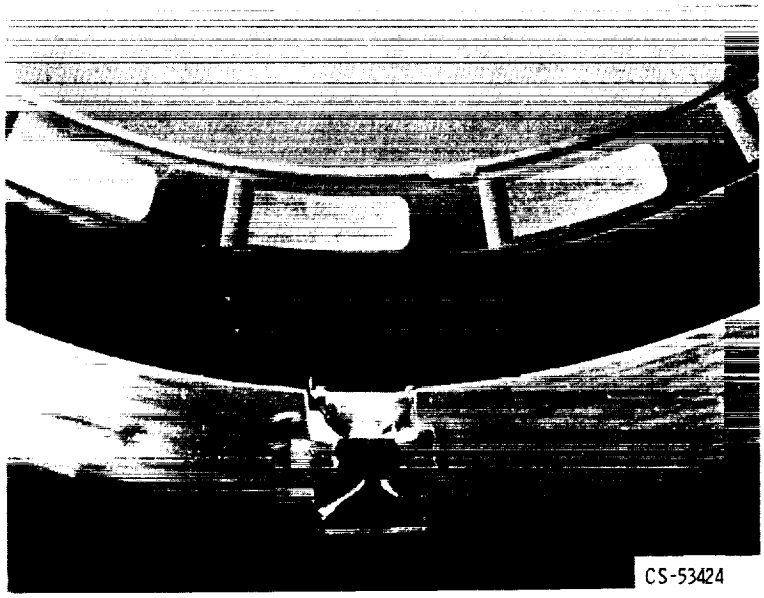

Figure 13. - Close-up of carbon nosepiece of the gas-film seal after 200 hours of endurance testing. Total time on seal: 338.5 hours.